Available online at www.sciencedirect.com
SCIENCE DIRECT®

Journal of the European Ceramic Society 24 (2004) 1233–1236

www.elsevier.com/locate/jeurceramsoc

Production of NTCR thermistor devices based on $NiMn_2O_{4+\delta}$

R. Schmidt, A. Basu, A.W. Brinkman*

University of Durham, Department of Physics, South Road, Durham DH1 3LE, UK

Abstract

$NiMn_2O_{4+\delta}$ ceramics exhibit a logarithmic increase of resistance with decreasing temperature (NTCR), which makes the compound well suited for use as a thermistor material in temperature sensing applications. In bulk material there are often problems with poor stability and reproducibility due to incomplete intergranular contact. These difficulties can be minimised in even and dense polycrystalline films. Screen-printing, electron-beam evaporation and rf magnetron sputtering processes have been developed for the production of thin and thick film NTCR thermistor devices. The source powder production, the experimental set-up, the process parameters and the resulting film properties for each of the processes are presented and compared. The surface topology was examined by scanning-electron microscopy (SEM) and atomic force microscopy (AFM). The phase purity of the source powder and the films was assessed by X-ray diffractometry (XRD). The electrical properties were analysed by measuring the resistance - temperature characteristics. This study suggests that rf magnetron sputtering processes are most advantageous.

Keywords: Electron-beam evaporation; Screen-printing; Spinels; Sputtering; Thermistors

1. Introduction

$NiMn_2O_{4+\delta}$ crystallises in a typical cubic spinel structure where the oxygen atoms form a fcc sublattice in a cubic-closed packed formation. The metal cations are situated on tetrahedral and octahedral lattice interstices.

In a regular spinel divalent cations are situated on tetrahedral and trivalent cations on octahedral sites. Conversely, in a complete inverse spinel structure all divalent cations move to octahedral sites. $NiMn_2O_{4+\delta}$ is an intermediate type of spinel where part of the Ni^{2+} cations transfer to octahedral sites, the Mn^{3+} cations on octahedral sites dis-proportionate to Mn^{2+} and Mn^{4+} and the Mn^{2+} cations move to the tetrahedral sites to compensate all Ni^{2+} vacancies. However, depending on the ambient and the temperature during the production process of $NiMn_2O_{4+\delta}$ materials, the oxygen content can vary and the cation distribution is then described by:

$$Ni^{2+}_{1-x}Mn^{2+}_{x}\left[Ni^{2+}_{x}Mn^{3+}_{2-2x-2\delta}Mn^{4+}_{x+2\delta}\right]O_{4+\delta}$$

where the [ ] brackets indicate octahedral sites.

Electrical conduction in $NiMn_2O_{4+\delta}$ is based on a thermally activated hopping mechanism where electrons transfer between Mn^{3+} and Mn^{4+} cations on octahedral sites. The d.c. conductivity follows a variable-range hopping model where the resistance decreases logarithmically with increasing temperature (NTCR). This makes the compound well suited for use as a thermistor material.

$NiMn_2O_{4+\delta}$ has been widely used in industry as a temperature sensor in bulk material applications, but problems with poor stability and reproducibility of the sensor due to high porosity and incomplete intergranular contact occur. Pores make the device sensitive to effects of the surrounding ambient such as changes in humidity, which affect the resistivity, or variations in oxygen partial pressure that change the oxygen content of the sensor material. These difficulties can be minimised in even and dense polycrystalline films. Thin $NiMn_2O_{4+\delta}$ films have been produced by electron-beam evaporation[1] and rf magnetron sputtering. Thick films were produced by screen-printing procedures.[2] In this paper the features, advantages and problems of these methods are reviewed and compared in terms of the resulting film properties.

* Corresponding author. Fax: +44-191-374-7358.
E-mail address: a.w.brinkman@durham.ac.uk (A.W. Brinkman).

0955-2219/03/$ - see front matter © 2003 Elsevier Ltd. All rights reserved.
doi:10.1016/S0955-2219(03)00415-1

2. Experimental

2.1. Powder production

$NiMn_2O_{4+\delta}$ source powder was produced by firing the precursor oxides NiO and Mn_2O_3 for 24 h at 1200 °C. The cubic $NiMn_2O_{4+\delta}$ spinel is stable only between 750 and 900 °C. Therefore, an annealing process at 800 °C for 50 h was necessary in order to restore phase purity. The composition of $NiMn_2O_{4+\delta}$ at 800 °C was retained by quench cooling from this temperature. However, this extensive thermal treatment led to a large average grain size, which was not appropriate for the paste production for screen-printing procedures. Instead, $NiMn_2O_{4+\delta}$ was produced via co-precipitation of a nickel manganese oxalate $NiMn_2(C_2O_4)_3{\cdot}6H_2O$ compound in which the nickel manganese ratio was appropriate for forming $NiMn_2O_{4+\delta}$ by thermal decomposition at 850 °C for 30 min. In co-precipitated $NiMn_2(C_2O_4)_3{\cdot}6H_2O$ the distribution of nickel and manganese atoms is more homogeneous and less heat exposure is required for the atoms to form the $NiMn_2O_{4+\delta}$ compound by diffusion processes.

The phase purity for the powders produced by both processes was confirmed by XRD.

2.2. Electron-beam evaporation

Thin films (~1 to 2 μm) were deposited onto glass substrates by electron beam evaporation with a system shown in the schematic diagram in Fig. 1. Electrons emitted from a tungsten filament were accelerated through a variable high potential drop (H.V.) and focussed onto the source powder contained in a carbon crucible. The evaporation process was carried out at pressures of 10^{-2}–10^{-3} Pa. The films were grown on 1 mm thick glass substrates, which were heated to 100 °C during deposition.

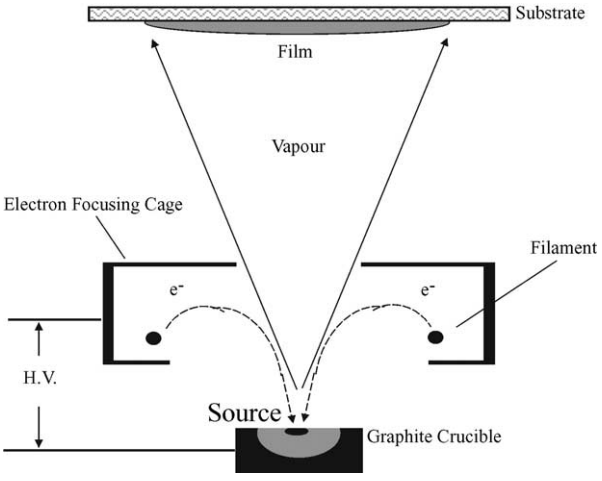

Fig. 1. Schematic diagram of the electron-beam system.

The source powder was produced via the mixed oxide route. The deposition time was about 30 min, the voltage applied between source and substrate 5 kV and the beam current 20 mA. The system exhibited a low average deposition rate of about 0.8 nm s^{-1}. After deposition the films showed poor crystallinity and were annealed at 850 °C for 10 min. The crystallinity could be improved significantly in this way.

2.3. Screen-printing

Thick films (~20 μm) were printed onto alumina substrates by screen-printing procedures. The basic principle of the screen-printing process is shown in Fig. 2.

In order to produce an optimum printing paste (ink), resulting in dense and even $NiMn_2O_{4+\delta}$ films, several components had to be added to the source powder produced via the oxalate route. The powder was mixed with a glass phase and an organic dispersing agent. Next, a "vehicle" containing organic solvents and organic binder was added. The paste was dispersed and printed onto thick film quality alumina substrates using a manual screen-printer equipped with a 115 T-mesh polyester screen. The paste was pressed through the screen onto the substrate by applying a print stroke with a squeegee blade. All the organic components were decomposed after printing the films during a sintering process at 850 °C for 30 min. The sintering process could also achieve a densification of the films and a good adhesion to the substrates.

The paste composition, paste viscosity, snap-off distance (gap) and the sintering process after the printing were all optimised to produce uniform, dense and even films in a regular printing process.

2.4. Rf magnetron sputtering

Thin films (~600 to 700 nm) were grown in a custom built on-axis rf magnetron sputtering system (Fig. 3).

Films were deposited by using a target made from the mixed oxide route. The powder was pressed into 2–3

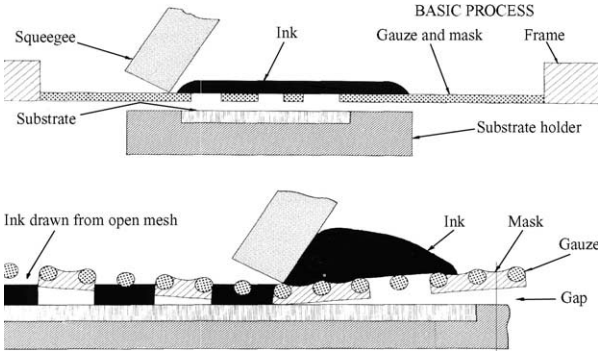

Fig. 2. Screen-printing process.

mm thick, 35 mm diameter discs and the discs were sintered, polished and fitted to a 33-cm diameter rf magnetron cathode using a heat conductive compound. The chamber was evacuated to a pressure of around 1.5×10^{-6} mbar before backfilling with argon to about 5×10^{-2} mbar for sputtering. The layers were deposited with a target power density of 3 watts cm^{-2}, on <100> silicon substrates. The substrate temperature was maintained at 200 °C during sputtering. The films were then annealed in air at 800 °C for 1 h to improve crystallisation followed by quenching to room temperature.

3. Results

All three types of film were examined with XRD. The phase purity of all the films lay within the limit of 3 wt.% resolution of the XRD analysis. The XRD patterns are shown in Fig. 4.

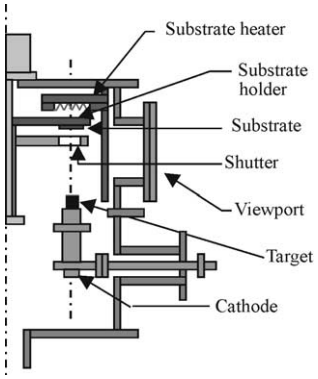

Fig. 3. Basic principle of rf magnetron sputtering.

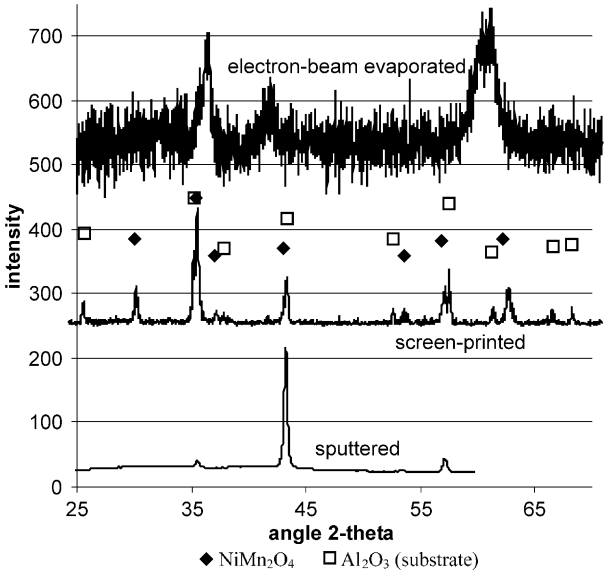

Fig. 4. XRD pattern of electron-beam evaporated, screen-printed and sputtered films, ◆ = $NiMn_2O_4$; □ = Al_2O_3 (substrate).

It can be seen that the thin electron-beam evaporated and the sputtered films had a strong preferred crystal orientation.

The surface topology of the films was assessed by SEM and AFM. As-deposited films grown by electron-beam evaporated and rf magnetron sputtering showed poor crystallinity on the surface, but adopted a more crystalline character after annealing. The microscope images of the annealed films and the sintered screen-printed film are presented in Fig. 5a–c.

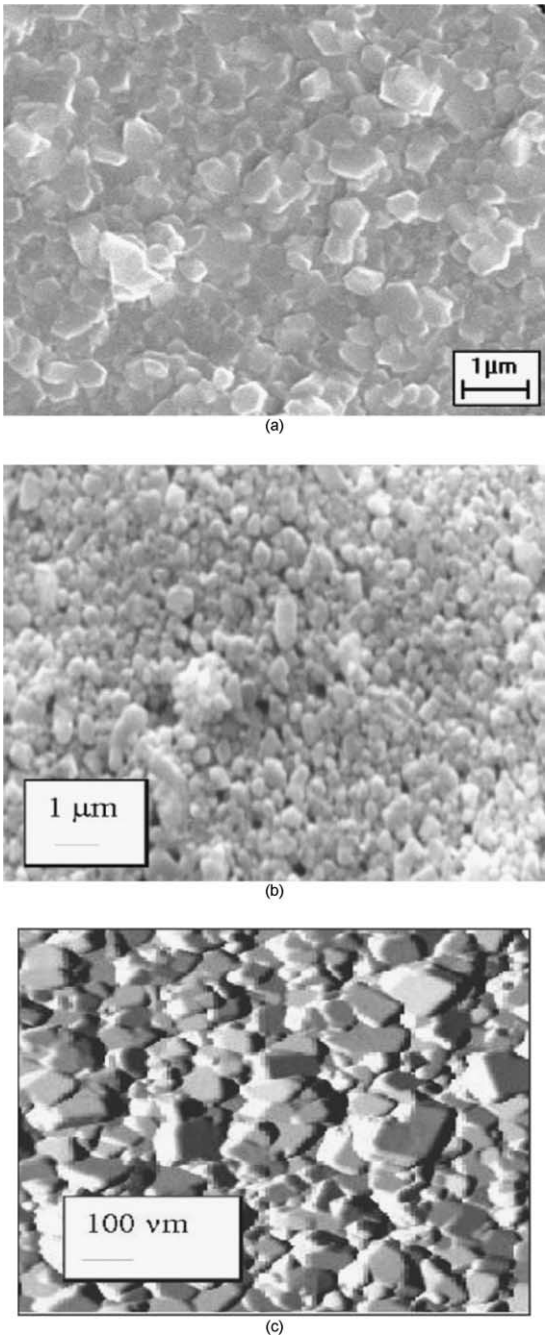

Fig. 5. (a) SEM image of an e-beam evaporated film, (b) AFM image of a sputtered film, (c) SEM image of a screen-printed film.

From Fig. 5 it can be seen that the screen-printed film had few holes and pores, in contrast to the electron-beam and sputtered films.

The sputtered film showed a superior crystallinity compared to the electron-beam evaporated film, which may be due to the longer annealing time of the sputtered film.

The Ni–Mn ratio of the films was analysed by an energy dispersive analysis of X-rays (EDAX) facility in the electron microscope. The films deposited by electron-beam evaporation were found to be nickel rich, implying that stoichiometry was not preserved during the process of sublimation, i.e. Ni was evaporated preferentially. Contrarily, the stoichiometry was correct in sputtered films and it was correct in screen-printed films logically.

The electrical properties of the films were characterised by measuring the variation of resistance with temperature. The resistance–temperature characteristics were consistent with the variable-range hopping model suggested by Mansfield:[3]

$$R = CT\exp\left(\frac{T_0}{T}\right)^{0.5} \quad (1)$$

where C is a constant, T the temperature and T_0 the characteristic temperature. T_0 can be determined by plotting $\ln(R^*T^{-1})$ vs. $1/T^{0.5}$ and the slope of the graph gives T_0. For the electron-beam evaporated film T_0 was found to be $T_0 = 2.23\times10^5$ K, for the screen-printed film $T_0 = 1.92\times10^5$ K and for the sputtered film $T_0 = 2.73\times10^5$ K. The slopes were all in a similar range, which indicates that the same variable-range hopping model of Eq. (1) occurs in all three types of film.

4. Discussion

The above results showed that electron-beam evaporation is an appropriate method to grow thin films with a good surface density (Fig. 5a). The source powder production was relatively simple. The film thickness was reproducible and could be controlled by adjusting the beam current by altering the potential drop and the filament current, the distance of source, filament and substrate and the deposition time. To improve crystallinity annealing was necessary but there was poor control on the crystal orientation in the films. The electrical properties were hardly reproducible either. The EDAX measurements showed that the stoichiometry in the films could not be controlled easily which was a major drawback with the electron-beam evaporation system used.

This problem was not encountered with screen-printing as it is a direct printing technique. The stoichiometry is maintained as the source powder is printed at room temperature, dispersed in a paste. Screen-printing is a very well established technique and no major technical challenges are involved with the design of the screen-printing kit. The film morphology and the electrical properties showed a very good reproducibility.

The drawback with screen-printing techniques was that the source powder and paste preparation were time intensive processes. Furthermore, the SEM picture (Fig. 5b) showed that the porosity of the films needed improvement to realise applications as temperature sensing device. It is believed that a more careful adjustment of the glass content in the material and the sintering process after printing would be necessary.

Contrarily, rf magnetron sputtered films showed good surface density (Fig. 5c), and the stoichiometry could be controlled. The average grain size was extremely small and most film properties could be controlled by adjusting the process parameters. The film thickness was controlled by adjusting the deposition time, the target–substrate distance and the power density on the target. The crystal orientation in the films was related to the substrate temperature during deposition.

Drawbacks of this technique were the difficult target preparation, low deposition rate and the annealing process, which was necessary to improve crystallinity.

5. Conclusion

It can be concluded that rf magnetron sputtering enables the best control on the film properties and no major problems occurred. Electron-beam evaporation was lacking control of film stoichiometry and screen-printing procedures would have to be further developed to improve the surface density.

Acknowledgements

The authors wish to thank Professor Dr. A. Roosen and Dipl Ing. A Stiegelschmitt for guidance developing screen-printing procedures.

References

1. Schmidt, R. and Brinkman, A. W., Preparation and characterisation of $NiMn_2O_4$ films. *International Journal of Inorganic Materials*, 2001, **3**, 1215–1217.
2. Schmidt, R., Stiegelschmitt, A., Roosen, A. and Brinkman, A. W., Preparation and performance of thick film NTC thermistors. *Key Engineering Materials, 7th Euroceramics*, 2002, **206–213**, 1417–1420.
3. Mansfield, R., Hopping conduction in III–V compounds. In *Hopping Transport in Solids*, ed. M. Pollak and B. Shklovskii. Elsevier Science, Amsterdam, 1991.